Distinct roles of the human cuneiform and pedunculopontine nuclei in gait and freezing of gait

Mathieu Yeche,[1,†] Antoine Collomb-Clerc,[1,2,†] Katia Lehongre,[1] Julie Bourilhon,[1,3] Yannick Mullié,[1] Nathalie George,[1] David Grabli,[1,4] Huiling Tan,[5] Nicolas Tempier,[1] Marco Romanato,[1] Claire Olivier,[1] Hayat Belaid,[1,6] Brian Lau,[1] Carine Karachi[1,6] and Marie-Laure Welter[1,3]

[†]**These authors contributed equally to this work.**

Abstract

Freezing of gait (FOG) in Parkinson's disease (PD) is a major cause of disability, often resistant to dopaminergic therapy and deep brain stimulation (DBS). Its underlying neural mechanisms remain unclear. The mesencephalic locomotor region (MLR) is a critical hub for gait control and a therapeutic target for DBS, but the respective functional roles of its two main nuclei, i.e. the cuneiform nucleus (CuN) and the pedunculopontine nucleus (PPN), remain unclear in human gait.

Here, we combined local field potential recordings from both the CuN and PPN with detailed biomechanical analyses of gait initiation in four PD patients suffering from dopa-resistant FOG. Neural activity was aligned to anticipatory postural adjustments (APA) and step execution to characterize the temporal organization of MLR dynamics during gait initiation and to identify alterations preceding freezing episodes. We also examined the effects of CuN, PPN and sham stimulation on gait initiation.

During gait initiation, the CuN and PPN exhibited distinct temporal and spectral neuronal activity patterns associated with different phases of gait initiation. Alpha-band activity in the CuN increased prior to APA and correlated with stepping rhythm, whereas the PPN showed prominent beta-band desynchronization during postural adjustments followed by alpha modulation during step execution. When FOG occurred after gait initiation (FOG+ trials, n = 38), we observed a breakdown of this spatiotemporal organization. Specifically, freezing was preceded by exaggerated and mistimed alpha-band synchronization across the MLR and abnormal modulation of PPN beta activity compared with non-freezing trials (FOG− trials, n = 115, $p < 0.05$). CuN stimulation selectively improved gait rhythm, whereas

PPN stimulation worsened forward propulsion. Across patients, excessive mesencephalic alpha activity predicted impaired gait initiation and reduced responsiveness to stimulation.

Together, these findings reveal a functional dissociation within the human MLR, with CuN activity linked to rhythmic step preparation and PPN activity associated with postural and execution-related processes, and subsequent FOG was associated with disruption of MLR dynamics during gait initiation, rather than a uniform loss of locomotor drive. By clarifying the distinct roles of the CuN and PPN and identifying frequency-specific biomarkers associated with gait failure, this study provides a mechanistic framework for understanding variable outcomes of MLR-DBS and supports the development of spatially and temporally adaptive neuromodulation strategies for gait disorders.

Author affiliations:

1 Sorbonne Université, Institut du Cerveau - Paris Brain Institute, Inserm, CNRS, AP-HP, Hôpital de la Pitié-Salpetrière, F-75013 Paris, France

2 NeuroX Institute and Brain Mind Institute, School of Life Sciences, Swiss Federal Institute of Technology (EPFL), 1015 Lausanne, Switzerland

3 Univ Rouen Normandie, Normandie Univ, CHU Rouen, Department of Neurophysiology, F-76000 Rouen, France

4 Department of Neurology, Hôpital de la Pitié-Salpetrière, AP-HP, F-75013 Paris, France

5 MRC Brain Network Dynamics Unit, University of Oxford, OX1 3TH, Oxford, UK

6 Department of Neurosurgery, Hôpital de la Pitié-Salpetrière, AP-HP, 75013 Paris, France

Correspondence to: Marie-Laure Welter

Paris Brain Institute, 47 bd de l'Hôpital, 75013 Paris, France

E-mail: marielaure.welter@icm-institute.org

Running title: MLR dynamics in gait and FOG

Keywords: cuneiform nucleus; pedunculopontine nucleus; mesencephalic locomotor region; freezing of gait; Parkinson's disease; human

Introduction

Freezing of gait (FOG) is a highly debilitating and poorly understood symptom of Parkinson's Disease (PD).[1,2] It is characterized by a sudden, transient inability to step effectively, leading to falls and loss of independence. It often shows a limited response to dopaminergic therapy and conventional deep brain stimulation (DBS). Recent anatomical, imaging, and physiological studies emphasize the brainstem mesencephalic locomotor region (MLR) as a critical hub for gait control[3–6] and a potential target for DBS in treating gait disorders and falls in PD.[7–10] However, clinical trials targeting the MLR have yielded inconsistent results,[10–14] highlighting the need to further understand the functional architecture of this complex region in humans.[15,16]

The MLR consists of two nuclei, without sharply defined anatomical boundaries: the ventral pedunculopontine nucleus (PPN) and the dorsal cuneiform nucleus (CuN). These nuclei exhibit distinct circuit integration profiles, suggesting divergent functions. The PPN is densely embedded within basal ganglia loops, receiving massive projections from basal ganglia outputs (the substantia nigra pars reticulata and the internal globus pallidus), and primarily integrates sensorimotor and associative information.[17–21] Its downstream influence is exerted through projections to the pontine reticular formation and ascending feedback loops to the thalamus. In contrast, the CuN receives weaker basal ganglia inputs, which are more restricted to limbic circuits (e.g., ventral striatum/pallidum). Furthermore, the CuN receives predominant inputs from threat-detection centers,[22,23] such as the inferior colliculus and the periaqueducal gray and sends excitatory projections to the medullary reticular formation (MRF),[5,17,24] positioning it to bypass finer postural control circuits and drive rapid, high-speed locomotion.[25] In mice, although the CuN contains both glutamatergic and gamma-aminobutyric acid (GABAergic) neurons,[19,21] optogenetic activation of the glutamatergic population is sufficient to drive high-speed locomotion.[4,26–28] The PPN comprises an even more heterogeneous population – including cholinergic, glutamatergic, and GABAergic neurons[6,25,29]– that modulates posture and exploration and can even halt locomotion, depending on the cell type activated.[19,21,29–31] In non-human primates, tonic and phasic-rhythmic neuronal activity are directly linked to locomotion, and increased burst activity is observed within the caudal MLR following dopaminergic depletion.[32] Furthermore, lesions of PPN cholinergic neurons cause specific locomotor and postural problems.[33]

In humans, there is limited direct evidence supporting a specific spatial organization of function.[34] Intraoperative recordings show that CuN neurons fired during simulated stepping,[35] and stimulation of this region can induce involuntary rhythmic leg muscle

activity.[36] At the same time, PPN local field potential (LFP) recordings reveal neural modulations during limb movements[37–39] and imagined gait,[40,41] and indicate that theta- and alpha-band activity are related to gait control.[42–44] Additionally, increased PPN-cortical alpha coherence has been observed during locomotion.[45] Critically, however, no previous study has recorded from both the CuN and PPN simultaneously to clarify their specific roles. As a result, it remains unknown whether MLR nuclei exhibit distinct electrophysiological signatures during locomotion and how these signatures relate to FOG.

This knowledge gap has clinical implications. Current MLR-DBS trials primarily target the PPN, but variability in the target and the unresolved contributions of the CuN versus PPN may explain the limited efficacy in treating FOG.[9,11–13,46,47] Furthermore, because FOG is an episodic phenomenon, standard continuous stimulation may fail to address the dynamic neural dysfunction preceding freezing episodes, which can be detected during gait initiation (GI).[48] To develop effective therapies, it is necessary to identify the specific temporal dynamics of MLR nuclei[49] during the transition from standing to walking, specifically distinguishing between anticipatory postural adjustments (APAs), which prepare balance, and the rhythmic stepping phase.

In this study, we used DBS electrodes implanted in the MLR, with contacts in both the CuN and PPN, to record LFPs in four PD patients with dopa-resistant FOG. By combining these recordings with biomechanical analyses of GI, we tested the hypothesis that the CuN and PPN have distinct, time-specific roles in human gait control. We identified electrophysiological signatures of subsequent freezing, encoded in specific frequency bands around GI, which predicted gait quality under DBS. These findings provide a potential mechanistic framework for understanding FOG development and could inform the design of future adaptive DBS strategies.

Materials and methods

Participants

Six patients with PD were enrolled in a randomized, cross-over controlled trial assessing the efficacy of MLR-DBS for gait and balance disorders, including FOG (see[13] for details). Eligibility criteria were: (1) diagnosis of idiopathic PD according to the United Kingdom Parkinson's Disease Society Brain Bank criteria; (2) age 18–70 years; (3) presence of gait and/or balance impairment not responsive to dopaminergic treatment, defined as a score >1 on the Movement Disorder Society–Unified Parkinson's Disease Rating Scale (MDS-UPDRS) part II (item 2.12, walking/balance, and/or item 2.13, freezing of gait) and/or part III (item 3.11, freezing of gait, and/or item 3.12, postural instability)[50] in the ON dopamine

medication state; (4) levodopa responsiveness >40% for other motor symptoms; (5) no contraindication to MRI or DBS surgery; (6) absence of dementia (Mattis Dementia Rating Scale score >129); (7) stable antiparkinsonian medication for ≥3 months before enrolment; (8) willingness to participate; and (9) written informed consent and social security affiliation. The study was conducted in accordance with the Declaration of Helsinki and Good Clinical Practice guidelines. Approval was obtained from the local ethics committee (Comité de Protection des Personnes, Ile-de-France VI), and the trial was registered at ClinicalTrials.gov (NCT02931097).

Surgical procedure, anatomical localization of recordings and stimulation of the MLR

At baseline, patients underwent a comprehensive clinical evaluation before bilateral implantation of MLR-DBS electrodes. Surgical MLR targeting was guided by preoperative 1.5T and 3T T1-weighted MRI and an in-house 3D histological deformable atlas of the human brainstem (Supplementary Fig 1).[51] This atlas provides density maps of cholinergic and non-cholinergic neuronal populations within the MLR, based on high-resolution MRI (11.7T) combined with immunohistochemical studies across several post-mortem human brainstems, with probabilistic delineation of the PPN, located at the level of the pontomesencephalic junction (PMJ), and the more dorsal CuN (Fig. 1A), consistent with previous histological studies of the human MLR.[15] This atlas was nonlinearly registered to each patient's preoperative T1 MRI, allowing patient-specific reconstruction of the MLR anatomy and used for surgical targeting (Supplementary Fig. 1). Intraoperative microelectrode recordings were performed on each side, under sedation in 3 patients and under general anaesthesia in one patient. According to per-operative physiological and anatomical checks using X-ray fluoroscopy, the 8-contact DBS leads (DB-2201, outer diameter 1.3 mm, contact height 1.5 mm, center-to-center spacing between adjacent contacts 2 mm, Boston Scientific) were implanted bilaterally and temporarily connected to externalized cables to allow LFP recordings. The electrodes were intentionally implanted along an oblique anteroposterior and dorsoventral trajectory spanning both nuclei. Contacts assigned to the PPN were located deeper along the leads, whereas those assigned to the CuN were located more dorsally. Due to both the anatomical organisation of the MLR and the oblique trajectory of implantation, CuN contacts were anterior to PPN contacts in stereotactic space. A post-operative 3D helical CT-scan was performed the day after surgery to check the absence of complications, co-registered with the preoperative T1-weighted MRI and overlaid on the MLR histological atlas to confirm lead position,

enabling reconstruction of electrode contacts relative to the CuN and PPN territories (Fig. 1A).

LFP recordings were acquired 1–4 days postoperatively before the pulse generator (Vercise PC, Boston Scientific) implantation, with recording dipoles defined as the midpoint between each contact pair (Fig. 1B). Fifteen dipoles were assigned to the CuN and 13 to the PPN subregions and included in subsequent analyses (Fig. 1B-D). This approach allowed us to include and dissociate contacts assigned to the atlas-defined PPN/CuN territories for both LFP recordings and DBS, for all patients (Fig. 1).

CuN stimulation (DBS^{CuN}), PPN stimulation (DBS^{PPN}) and sham stimulation (DBS^{OFF}) were tested 2 months after surgery, each applied for a 2-month period, in a cross-over randomized order with double-blind assessments (see[13]). We used bipolar DBS using adjacent contact as anode and cathode, for both CuN and PPN targets with 30 Hz stimulation frequency, 60 μs pulse width and 1.7 to 4.2 mA amplitude (Supplementary Table 1). Amplitudes were individually selected below side-effect threshold and kept constant within each stimulation condition. The mean coordinates of the stimulating contacts (mm) relative to the midline (X, lateral), fourth ventricle (Y, anteroposterior) and PMJ (Z, depth, with negative values indicating electrodes placed below the PMJ) were for CuN DBS: X, Y and Z = 8.5, 9.2 and 3.6 mm, respectively, and for PPN DBS: X, Y and Z = 6.5, 6.9 and -1.1 mm (Fig. 1, Supplementary Table 1).

Gait initiation recordings

Patients underwent biomechanical and physiological gait assessments across four sessions in the Paris Brain Institute Physiology and Analysis of Movement (PANAM) core facility. In each session, patients were tested in two conditions: without dopaminergic medication ($DOPA^{OFF}$, following a 12-h withdrawal) and with dopaminergic medication ($DOPA^{ON}$, after administration of a suprathreshold levodopa dose equal to the usual morning intake plus 50 mg). The first session occurred 1–4 days postoperatively, allowing coupling with MLR-LFP recordings (Fig. 2A). Two patients were unable to perform this postoperative session due to fatigue, and MLR-LFP were obtained in four patients (Fig. 1). The four patients completed 153 trials, during which all exhibited freezing with 38 FOG episodes recorded (Supplementary Table 2).

The following sessions were performed under CuN stimulation (DBS^{CuN}), PPN stimulation (DBS^{PPN}), or sham stimulation (DBS^{OFF}) (Fig. 1).

Gait initiation (GI) was recorded using a 0.9 × 1.8 m force platform (AMTI, Watertown, MA, USA). Each trial began with quiet standing until a visual cue signaled the start of walking; patients then walked straight for 6–8 m, turned, and returned to the platform. Ground reaction forces and moments were sampled at 1000 Hz. Whole-body kinematics during straight walking and turning were acquired with a 32-marker motion capture system (Vicon®, Oxford, UK). Bilateral surface EMG recordings of the soleus and tibialis anterior muscles were sampled at 2000 Hz (Fig. 2A). The severity of axial motor symptoms was assessed using the MDS-UPDRS part III axial subscore (sum of items: speech, arising from chair, gait, freezing of gait, postural stability, posture)[50] and the Gait and Balance Scale (GABS)[52] (Supplementary Table 2).

Gait initiation parameters and FOG events

Gait initiation was segmented into two phases: (1) anticipatory postural adjustments (APA), from the initial biomechanical event (t_0) to foot-off of the leading limb (FO_1); and (2) step execution, from FO_1 to the first foot contact. Seventeen spatiotemporal GI parameters were extracted for each trial from ground reaction forces and moments along the mediolateral (x), anteroposterior (y), and vertical (z) axes (Fig. 2A, Supplementary Fig. 2). Trials in which t_0 could not be reliably identified were excluded from analysis. FOG episodes were annotated from motion capture and EMGs recordings, defined as a transient inability to initiate or continue stepping which bursty co-contractions of antagonist muscles (Fig. 2B, Supplementary video). Each episode was marked online during acquisition and subsequently verified offline by two independent raters. Gait initiation trials were classified as FOG+ (containing at least one FOG episode) or FOG- (without FOG).

Gait initiation statistical analysis

The GI parameters extracted from force platform recordings were projected onto a varimax-rotated principal component analysis (RPC) space obtained in a previous cohort of 38 PD patients performing a similar task.[48] GI parameters were also compared to 24 age-matched healthy controls (HC) (see[48] for details) (Supplementary Fig. 2). In brief, we obtained 5 orthogonally RPC scores accounting for 73% of variance, each interpreted based on correlations with the original GI parameters using Pearson's correlation test. RPC1 related to forward stepping vigor and propulsion, which we labelled *Pace*; RPC2 reflected step times and cadence, which we labelled *Rhythm*; and RPC5 represented step width and lateral CoM speed, which we labelled *Lateral balance* (Supplementary Fig. 2)

We first examined how GI performance scores changed during post-operative gait trials using linear mixed-effect models (LMM) with FOG vunerability (FOG+ vs. FOG-) and dopaminergic medication ($DOPA^{OFF}$ vs. $DOPA^{ON}$) as predictors with full interaction and patients as a random effect. Then, we explored how GI RPC scores were modified across DBS conditions, using a LMM with dopaminergic medication ($DOPA^{OFF}$ vs. $DOPA^{ON}$) and DBS condition (DBS^{OFF} vs. DBS^{CuN} vs. DBS^{PPN}) as predictors with full interaction and patients as random effect. We report estimated regression coefficient (β) ± standard error and associated *p*-values. All statistical analyses were performed in R (v4.2.2) using the *lme4* and *emmeans* packages for LMMs. Bonferroni correction was applied for multiple comparisons (n=5 RPCs), and corrected *P*-values (P_c) < 0.05 were considered significant.

MLR-LFPs recordings

MLR-LFPs were acquired using bipolar montages constructed from seven adjacent contact pairs of the DBS lead (Boston Scientific Cartesia; contact diameter 1.3 mm, height 1.5 mm, inter-contact spacing 0.5 mm; ventral contact labeled 1, dorsal contact labeled 8). LFPs were recorded continuously during gait initiation and walking, amplified, band-pass filtered (0.25–300 Hz), sampled at 512 Hz, and wirelessly transmitted via Bluetooth to a recording computer through a portable amplifier (Porti 32, TMS International, Enschede, The Netherlands) carried in a small backpack worn by the patient (Fig. 2A). Kinetic signals from gait initiation and LFP activity were recorded simultaneously, synchronized, and exported for offline analysis using a MATLAB-based toolbox (MathWorks Inc.; http://biomechanical-toolkit.github.io). The implantable neurostimulator (Vercise PC, Boston Scientific) was placed the day after LFPs acquisition.

LFPs data processing

MLR-LFPs were digitally high-pass filtered at 1 Hz, notch filtered at 50 Hz, and epoched from 2 s before the cue to the end of the second swing phase. Time–frequency decomposition was performed using a multitaper spectral estimation algorithm (Chronux toolbox, http://chronux.org/) with three orthogonal tapers and a 500 ms sliding window advanced in 30 ms steps. Power spectra (1–50 Hz) were baseline normalized to an 800 ms pre-trial period and expressed in decibels ($10 \times \log_{10}$). Time–frequency representations were screened for transient artifacts. Trials were excluded if mean power exceeded 5.7-fold baseline or if peak power exceeded 7.5 dB within –0.5 to +0.5 s from gait initiation onset (1–100 Hz range). In addition, all trials were visually inspected by at least two independent examiners for saturation, spectral smearing, and movement- or cable-induced artifacts.

LFPs data statistical analysis

We examined changes in MLR-LFPs during GI by applying a LMM at each point of the time-frequency map, using FOG imminence (FOG- vs. FOG+ trials, Fig. 2B), dopaminergic medication ($DOPA^{OFF}$ vs. $DOPA^{ON}$) and localization (PPN vs. CuN) as predictors with full interactions, and recording dipole nested within subjects as random effect. After identifying clusters of interest, we applied the same LMM in 500-ms time windows within defined frequency bands (alpha: 8-12 Hz; low-beta: 13-20 Hz; high-beta: 20-35 Hz). We then followed the same logic to examine, for each RPC, the relationship between MLR-LFPs and RPC scores. To do so, we added the RPC score as an interacting continuous predictor to the previous LMMs. We report the estimated regression coefficient (β) ± standard error and associated *p*-values. All statistical analyses were performed in R (v4.2.2) using the *lme4* and *emmeans* packages for LMMs. We corrected for multiple comparisons to control the false discovery rate and considered adjusted *P*-values < 0.05 as significant.

For regressions of post operative LFP power and *Rhythm* with DBS, we performed a linear regression with *Rhythm* score and localization/DBS condition (PPN vs. CuN) as fully interacting factors. A bonferroni correction was applied for multiple comparisons (n=5 RPCs), and corrected *P*-values (P_c) < 0.05 were considered significant.

Results

Specific CuN and PPN neuronal activity

We recorded LFPs from the MLR of four patients with advanced PD during self-initiated gait, alongside force platform, motion capture, and electromyography (Fig. 2A, Supplementary Table 2, Supplementary Fig. 2). A total of 56 bipolar LFP recordings (7 per electrode; one electrode per hemisphere, Supplementary Fig. 3) were localized using a histology-based human brainstem atlas[13,51]. Of these, 13 dipoles were localized in the PPN (cholinergic population) and 15 in the CuN, with each patient contributing at least one dipole in both nuclei (Fig. 1B-D, Supplementary Fig. 3).

Baseline (standing still) activity showed higher low-beta (13–20 Hz) power in the PPN than in CuN ($t_{(3)}$ = –3.46, P = 0.041), whereas alpha (8–12 Hz) power did not differ significantly ($t_{(3)}$ = –2.00, P = 0.14; Fig. 2C). Under dopaminergic medication, baseline MLR LFP activity was not significantly modified (e.g., beta power: $t_{(3)}$ = 0.86, P = 0.45), although one participant showed a marked reduction in PPN beta-band activity $DOPA^{ON}$ vs $DOPA^{OFF}$ conditions

(Supplementary Fig. 4A). During GI, dopaminergic medication did not induce significant changes in MLR alpha or beta power (Supplementary Fig. 2B-C), with a smaller theta increase during APAs in the CuN ($DOPA^{OFF}$ vs. $DOPA^{ON}$: 0.13 to 0.64 s, β = 1.85 ± 0.48 dB, P = 0.0001, Supplementary Fig. 4C-D). Given the absence of alpha and beta modulations between dopaminergic medication conditions, we pooled LFP data from both DOPA states in subsequent analyses, keeping medication condition as a covariate.

Gait initiation is altered by FOG imminence

All four PD patients experienced FOG during the session, yielding 38 FOG trials (FOG+; 12 $DOPA^{OFF}$, 26 $DOPA^{ON}$), with FOG occurring on average 13.5 steps after GI (IQR, 10–23), during walking or turning (Supplementary video). We also collected 115 trials without FOG episodes (FOG−; 57 $DOPA^{OFF}$, 58 $DOPA^{ON}$).

We compared GI parameters across FOG+ and FOG- trials, and between $DOPA^{OFF}$ and $DOPA^{ON}$ conditions using principal component scores: *Pace* (correlating with step length, propulsion and stepping vigor), *Rhythm* (correlating with step timing and cadence), and *Lateral balance* (correlating with step width and lateral center of mass velocity) (Fig. 2D, Supplementary Fig. 2). *Pace* was unaffected by either FOG imminence (β = 0.0039 ± 0.068 a.u., P_c = 0.99) or dopaminergic medication (β = 0.047 ± 0.056 a.u., P_c = 0.99, Fig. 1d). *Rhythm*, by contrast, was significantly impaired when FOG was imminent (FOG+ vs FOG- trials; β = 0.63 ± 0.16 a.u., P_c < 0.001), with a stronger effect in the $DOPA^{OFF}$ state ($DOPA^{OFF}$ vs $DOPA^{ON}$; β = 1.08 ± 0.28 a.u., P_c < 0.001; Fig. 2D, Supplementary Fig. 2). *Lateral balance* did not significantly differ between FOG+ and FOG- trials (FOG+ vs FOG- trials; β = -0.057 ± 0.086 a.u., P_c > 0.99) but was significantly deteriorated under dopaminergic medication (β = 0.40 ± 0.07 a.u., P_c < 0.001), with a more pronounced effect in FOG+ trials (β = –0.33 ± 0.15 a.u., P_c = 0.026; Fig. 2D, Supplementary Fig. 2). In FOG+ trials, dopaminergic medication exerted opposite effects, enhancing *Rhythm* (β =-1.07 ± 0.24 a.u., P_c < 0.001) while worsening *Lateral balance* (β = 0.56 ± 0.13 a.u., P_c < 0.001; Fig. 2D).

Together, these findings demonstrate that impaired *Rhythm* and *Lateral balance* during GI are key markers of FOG imminence in PD. Dopaminergic medication amplified their dissociation by partially rescuing *Rhythm* but impairing *Lateral balance*.

Specific contribution of CuN and PPN neural dynamics during GI

Examining LFP activity during GI, irrespective of FOG imminence, CuN and PPN exhibited distinct patterns (Fig. 3A, Supplementary Fig. 4A). In the CuN, alpha-band power increased

before APAs onset (Fig. 3B-C). In the PPN, pronounced beta-band desynchronization occurred during APAs, with alpha-band activity rising afterward (during gait execution) (Fig. 3B-C). Direct time-frequency comparisons confirmed these differences: the pre-APA alpha increase was stronger in the CuN (-0.35 s to 0.04 s, β = 1.22 ± 0.36 dB, P = 0.0026), whereas post-APA low-beta desynchronization was stronger in the PPN (-0.17 s to 0.40 s, β = 0.88 ± 0.25 dB, P = 0.0012; Fig. 3B-C, Supplementary Fig. 5A).

FOG imminence dissociates CuN and PPN neural encoding of GI

To further understand how MLR neuronal activity is shaped by FOG imminence, we compared LFP between FOG+ and FOG− trials, in both nuclei (Fig. 4A). When FOG was imminent, pre-APA alpha-band power tended to decrease in the CuN (FOG+ vs. FOG- trials, -0.3 s to 0 s, β = 0.39 ± 0.39, P = 0.3132, Fig. 4B, Supplementary Fig. 5B and Supplementary Fig. 6). Conversely, per-APA alpha-band power significantly increased in both the CuN and PPN for FOG+ trials (FOG+ vs. FOG- trials, 0.04 s to 0.67 s, β = 1.09 ± 0.29 dB, P = 0.0002, Fig. 4A-B, Supplementary Fig. 5B and Supplementary Fig. 6) with no significant differences between MLR subregions (FOG+ trials: CuN vs PPN, 0.04 s to 0.67 s, β = 0.11 ± 0.56 dB, P = 0.84, Fig 5B-C; Supplementary Fig. 5B and Supplementary Fig. 6). In the PPN, low-beta desynchronization was significantly stronger for FOG+ trials compared to FOG- trials (0.43 s to 0.67 s, β = 1.09 ± 0.44 dB, P = 0.0137; Fig. 4A-C, Supplementary Fig. 5B and Supplementary Fig. 6).

Looking at the correlation between MLR-LFP and GI performance, we found that CuN alpha-band power at APA onset significantly positively correlated with *Rhythm* and *Lateral balance* scores (*Rhythm* : -0.23 s to 0.16 s, β = 0.73 ± 0.21 dB, P = 0.0005; *Balance*: -0.08 s to 0.19 s, β = 1.33 ± 0.39 dB, P = 0.0006, Fig. 5). In the PPN, alpha-band power at APA onset negatively correlated with *Pace* (-0.11 s to 0.16 s, β = -1.50 ± 0.47 dB, P = 0.002), and with *Rhythm* at the end of APA (time of FO1, 0.43 s to 0.70 s, β = –0.90 ± 0.30 dB, P = 0.0041; Fig. 5B). We found no significant correlation between gait scores and low-beta modulation (Supplementary Fig. 7).

Together, these results indicate that early CuN alpha activity supports *Rhythm* and *Balance* at GI, but exaggerated alpha activity during APAs phase across the MLR disrupts GI with FOG imminence, with additional lowered low-beta PPN activity.

CuN-DBS improves Rhythm in relationship with alpha band power

We assessed the effects of DBS of the CuN (DBS^{CuN}) or PPN (DBS^{PPN}) relative to no stimulation (DBS^{OFF}) using a double-blind, randomized design (Fig. 6 A, Supplementary Fig. 8).

DBS^{PPN} significantly worsened *Pace* compared with both DBS^{OFF} and DBS^{CuN} (DBS^{PPN} vs. DBS^{OFF}: $\beta = 0.30 \pm 0.04$, $P_c < 0.001$; DBS^{PPN} vs. DBS^{CuN}: $\beta = -0.20 \pm 0.04$, $P_c < 0.001$; Fig. 6A), whereas DBS^{CuN} had no significant effect (DBS^{CuN} vs. DBS^{OFF}, $\beta = 0.10 \pm 0.04$, $P_c = 0.11$). In contrast, DBS^{CuN} significantly improved *Rhythm* compared with DBS^{OFF} (DBS^{CuN} vs. DBS^{OFF}: $\beta = -0.27 \pm 0.08$, $P_c = 0.0023$; Fig. 6A), whereas DBS^{PPN} had no significant effect (DBS^{PPN} vs. DBS^{OFF}: $\beta = -0.086 \pm 0.076$, $P_c = 1.00$; DBS^{PPN} vs. DBS^{CuN}: $\beta = -0.18 \pm 0.08$, $P_c = 0.083$; Fig. 6A). *Lateral balance* was not significantly affected by either DBS^{PPN} or DBS^{CuN} (DBS^{PPN} vs. DBS^{OFF}: $\beta = 0.073 \pm 0.066$, $P = 1.00$; DBS^{PPN} vs. DBS^{CuN}: $\beta = 0.042 \pm 0.066$, $P = 1.00$; Fig. 6A).

Across patients, alpha increases during APAs were negatively correlated with *Rhythm* under both DBS^{CuN} ($\beta = -4.26 \pm 0.59$ dB/au, $P = 0.0001$) and DBS^{PPN} ($\beta = -3.14 \pm 0.69$ dB/au, $P = 0.0019$) conditions (Fig. 6B). This relationship was significant in both FOG+ ($\beta = -5.21 \pm 0.64$ dB/au, $P < 0.0001$) and FOG− trials ($\beta = -2.18 \pm 0.64$ dB/au, $P = 0.0094$). These findings indicate that exaggerated alpha activity predicted a limited MLR DBS benefit for *Rhythm*.

Discussion

Our findings reveal distinct neural dynamics within the human MLR during gait initiation. By combining multisite LFP recordings with kinetic analysis, we observed temporally and spectrally different activity patterns in the CuN and PPN areas associated with specific phases of gait initiation. CuN alpha-band activity increased before APAs and correlated with subsequent stepping rhythmic, whereas PPN activity showed beta-band desynchronization during APAs followed by alpha modulation at step onset. Imminent FOG was characterized by disruption of this spatial and temporal organization, with abnormal alpha synchronization persisting during APAs and across the MLR, and increased beta modulation in the PPN. Interestingly, CuN-DBS selectively improves stepping rhythm, whereas PPN-DBS worsens forward vigor.

CuN alpha dynamics as the gait rhythm generator

In our study, CuN activity was distinguished from PPN activity by an early alpha-band peak that began well before APAs, decreased during APAs, and then increased again at liftoff of the lead foot. The magnitude of the pre-APA alpha activity correlated with the subsequent stepping rhythm, suggesting that CuN alpha dynamics are associated with the neural preparation for initiating locomotion and rhythm. This interpretation is consistent with experimental studies indicating that the CuN contributes to locomotor initiation.[6,53] While PPN shows no pre-APA alpha-band peak, it does show a surge in alpha-band activity at the start of stepping. The late surge in alpha-band activity observed in both the CuN and PPN areas, may relate to online locomotor control, consistent with MLR recordings linking theta-alpha power to walking speed in mice[54] and humans.[43,44]

This temporal and spectral organization was altered when freezing is imminent (i.e., after successful gait initiation by 13.5 steps). In these trials, the pre-APA CuN alpha-band modulation was attenuated and associated with deterioration of stepping rhythm. At the same time, the PPN alpha-band activity was no longer temporally aligned with step onset, suggesting a loss of functional specificity within the MLR. The disruption of CuN-PPN temporal alignment in the neural activity may reflect impaired transitions from APAs to step execution. One possible interpretation is that abnormal alpha-band synchronization reflects a breakdown of the distributed networks linking the MLR to cortical locomotor circuit, including cortical SMA-premotor regions.[55] Such network disruption could impair the essential alignment of postural preparation,[56–58] leading to impaired coordination between postural weight-shifting and step timing, some of the earliest signs of impeding FOG episodes.[59,60] These abnormalities may be particularly pronounced in cognitively demanding gait tasks that increase cortical engagement.[61,62] These data suggest that this loss of spatial and temporal precision in alpha-band activity could serve as an electrophysiological marker of early behavioral indicators of FOG,[44] such as irregular cadence and shorter step duration.[48,63,64]

PPN beta dynamics

In contrast to the CuN, the PPN showed significant low-beta desynchronization during APAs. This finding is consistent with previous report of beta suppression in the MLR during imagined gait,[41] voluntary leg movements,[65] and gait-phase transitions.[45] Anatomically, the PPN is more densely integrated with basal ganglia circuits than the CuN,[21] and displays functional beta-band coupling with the subthalamic nucleus (STN).[66,67] Similar decreases in beta power are observed within STN–cortical circuits during leg movements,[68] stepping

in place,[69,70] gait initiation,[48] and walking,[71] where they correlate with motor readiness and movement vigor.[72] Our findings thus support that PPN beta suppression during APAs may reflect engagement of neural mechanisms supporting postural readiness and step execution. Unexpectedly, trials with imminent FOG were associated with exaggerated low-beta desynchronization in the PPN. While high beta-band power is typically associated with antikinetic states in the SMA-premotor cortical areas and the STN,[73–76] recent studies have reported increased low-beta STN modulation in patients prone to FOG.[48] This pattern may reflect an increased recruitment of prefrontal-medial cortical circuits to compensate for reduced gait automaticity and impaired postural control.[75,77,78] Our findings suggest that the exaggerated PPN beta modulation observed here may reflect a similar compensatory response, with an attempt to recruit postural mechanisms when locomotor initiation becomes unstable due to concurrent alpha-band modulation in the CuN.

Dissociating clinical effects: CuN versus PPN stimulation

Our double-blind stimulation results obtained in the same patients provide consistent results with the distinct neural signature recorded in the two nuclei. CuN-DBS selectively improved stepping rhythm, whereas PPN-DBS paradoxically worsened pace, reducing step length and velocity. These observation are consistent with animals studies.[5,79] Activation of glutamatergic CuN neurons can initiate locomotion and drive high-speed locomotion with physiological stepping patterns in healthy animals,[4,19,29,80,81] restoring locomotion in Parkinsonian mice.[30,82] This effect likely relied on the rhythmic activation of descending reticulospinal projections.[17,24,83,84] Conversely, specific activation of PPN neurons in mice can halt locomotion or restrict it to slow, exploratory modes.[19,25,54,85]

These divergent outcomes may help explain the heterogeneous results reported in previous MLR-DBS trials, which predominantly targeted the PPN.[9,11,46,86] Our findings suggest that the therapeutic efficacy of MLR-DBS on FOG may depend on the precise modulation of specific MLR subregions and their associated locomotor circuits, with the preferential modulation of dorsal/posterior MLR circuits with rhythmic stepping while avoiding stimulation of the ventral PPN-related circuits that may interfere with forward propulsion.[36] This is supported by recent evidence that unilateral CuN stimulation promotes locomotor recovery in rodent models[87,88] and human spinal cord injury.[89]

Implications for Adaptive DBS

Our results also suggest a potential electrophysiological marker associated with freezing vulnerability and therapeutic resistance: exaggerated alpha-band synchronization across the MLR. This abnormal pattern was present across both nuclei and mirrored oscillatory abnormalities reported in the STN[48] in freezing-prone patients. This suggests that abnormal alpha synchronization may reflect a network-level disturbance affecting gait automaticity. This finding raises the possibility that abnormal alpha synchronization could provide a potential target for next-generation adaptive DBS (aDBS). Closed-loop DBS systems have already shown promise when targeting beta power in cortical-basal ganglia networks,[90,9192,93] our data suggest that monitoring pathological alpha dynamics within the MLR could provide a complementary approach specifically targeting locomotor dysfunction for alleviating freezing.[49] By dynamically modulating stimulation based on real-time alpha dynamics, aDBS could theoretically restore the temporal precision of gait initiation without the side-effect of continuous stimulation.

Limitations and perspectives

Several limitations should be considered. First, the rarity of human MLR recordings and the small number of patients inevitably limit generalizability. Second, DBS applied within the MLR can influence multiple neuronal population and neighboring structures and therefore cannot isolate nucleus-specific mechanisms. Rather than providing definitive causal evidence, the stimulation results should be considered supportive observations consistent with functional differentiation suggested by electrophysiological recordings. Third, because recordings were obtained through externalized leads during whole-body locomotion, movement- and cable-related artifacts precluded reliable analysis of LFP dynamics during continuous walking, turning, and of FOG episodes themselves. Here, we could not exclude the fact that differences in neural dynamics may also exist for FOG episodes occurring during turning, straight forward walking or at gait initiation. Future studies should expand these findings in animal models and incorporate multimodal recordings across basal ganglia, brainstem, and cortical networks to better characterize the distributed neural dynamics during the different locomotion phases, including continuous walking and turning, and its dysfunction in PD. Given the episodic, context-dependent nature of FOG and its sensitivity to stress or environmental triggers,[1,29,55,94] the role of limbic and sensory inputs to the MLR also merits further investigation.[22,23,95]

Conclusion

Our findings reveal distinct neural dynamics within the human MLR during gait initiation. Activity patterns in the CuN and PPN seem to play complementary yet distinct roles, respectively in the alpha- and low-beta bands spectrum. Disruption of this coordinated activity emerges as a possible neural mechanism underlying freezing, and alpha-band activity as a predictor of reduced DBS responsiveness. These results provide new insights into the neural organization of the MLR in human, with the CuN emerging as a potential surgical target and alpha-band as a physiological marker for guiding adaptive neurostimulation therapies to restore mobility in PD.

Data availability

Due to data protection regulations of Salpêtrière Hospital, INSERM and Paris Brain Institute, the raw gait and MLR LFPs data used in this study are available from the corresponding author (M.L.W) after approval of the IRB of these institutions. Source data are provided with this paper.

Acknowledgements

The authors sincerely thank our patients for their dedication in participating in this research. We are also grateful to the nurses of the Clinical Investigation Center at the Paris Brain Institute for their assistance in organizing the research program, to Angele Van Hamme and Déborah Ziri for their help in data recordings, to Eric Bardinet and Sara Fernandez-Vidal for imaging processing. The thumbnail image for the online table of contents was partially generated with ChatGPT, and modified by M.-L.W. using GIMP software.

Funding

This study was supported by the Institut National de la Recherche Médicale (INSERM) and the 'Investissements d'avenir' program (ANR-10-IAIHU-06 and ANR-11-INBS-0006) and grants from the Michael J Fox Foundation for Parkinson's disease (grant number: 10019). A.C.C. receives funding from European Union's Horizon 2020 research and innovation

program under the Marie Skłodowska-Curie grant (H2020-MSCA, grant agreement n°101034260) and the Swiss National Science Foundation (SNSF, EPFLeaders4impact); M.Y. receives support by the Paris Sorbonne University; Y.M receives funding from the European Union's Horizon 2020 research and innovation program under the Marie Slodowska-Curie-Horizon 2020 (H2020-MSCA-IF-2019, grant agreement No 898265).

Competing interests

The authors report no competing interests.

Supplementary material

Supplementary material is available at *Brain* online.

References

1. Nutt JG, Bloem BR, Giladi N, Hallett M, Horak FB, Nieuwboer A. Freezing of gait: moving forward on a mysterious clinical phenomenon. *Lancet Neurol*. 2011;10(8):734-744. doi:S1474-4422(11)70143-0 [pii] 10.1016/S1474-4422(11)70143-0

2. Fasano A, Aquino CC, Krauss JK, Honey CR, Bloem BR. Axial disability and deep brain stimulation in patients with Parkinson disease. *Nat Rev Neurol*. 2015;11(2):98-110. doi:nrneurol.2014.252 [pii] 10.1038/nrneurol.2014.252

3. Nielsen JB. How we walk: central control of muscle activity during human walking. *Neuroscientist*. 2003;9(3):195-204. doi:10.1177/1073858403009003012

4. Caggiano V, Leiras R, Goñi-Erro H, et al. Midbrain circuits that set locomotor speed and gait selection. *Nature*. Published online 2018. doi:10.1038/nature25448

5. Takakusaki K, Habaguchi T, Ohtinata-Sugimoto J, Saitoh K, Sakamoto T. Basal ganglia efferents to the brainstem centers controlling postural muscle tone and locomotion: a new concept for understanding motor disorders in basal ganglia dysfunction. *Neuroscience*. 2003;119(1):293-308.

6. Leiras R, Cregg JM, Kiehn O. Brainstem Circuits for Locomotion. *Annu Rev Neurosci*.

2022;45:63-85. doi:10.1146/annurev-neuro-082321-025137

7. Fling BW, Cohen RG, Mancini M, et al. Functional reorganization of the locomotor network in Parkinson patients with freezing of gait. *PLoS One*. 2014;9(6):e100291. doi:10.1371/journal.pone.0100291 PONE-D-14-12711 [pii]

8. Lench DH, Embry A, Hydar A, Hanlon CA, Revuelta G. Increased on-state cortico-mesencephalic functional connectivity in Parkinson disease with freezing of gait. *Parkinsonism Relat Disord*. 2020;72:31-36. doi:10.1016/j.parkreldis.2020.02.008

9. Golestanirad L, Elahi B, Graham SJ, Das S, Wald LL. Efficacy and Safety of Pedunculopontine Nuclei (PPN) Deep Brain Stimulation in the Treatment of Gait Disorders: A Meta-Analysis of Clinical Studies. *Can J Neurol Sci*. 2016;43(1):120-126. doi:10.1017/cjn.2015.318

10. Stefani A, Lozano AM, Peppe A, et al. Bilateral deep brain stimulation of the pedunculopontine and subthalamic nuclei in severe Parkinson's disease. *Brain*. 2007;130(6):1596-1607. doi:10.1093/brain/awl346

11. Ferraye MU, Debu B, Fraix V, et al. Effects of pedunculopontine nucleus area stimulation on gait disorders in Parkinson's disease. *Brain*. 2010;133(Pt 1):205-214. doi:awp229 [pii] 10.1093/brain/awp229

12. Welter ML, Demain A, Ewenczyk C, et al. PPNa-DBS for gait and balance disorders in Parkinson's disease: a double-blind, randomised study. *Journal of Neurology*. 2015;262(6). doi:10.1007/s00415-015-7744-1

13. Bourilhon J, Olivier C, You H, et al. Pedunculopontine and Cuneiform Nuclei Deep Brain Stimulation for Severe Gait and Balance Disorders in Parkinson's Disease: Interim Results from a Randomized Double-Blind Clinical Trial. *J Parkinsons Dis*. 2022;12(2):639-653. doi:10.3233/JPD-212793

14. Wang H, Gao H, Jiao T, Luo Z. A meta-analysis of the pedunculopontine nucleus deep-brain stimulation effects on Parkinson's disease. *Neuroreport*. 2016;27(18):1336-1344. doi:10.1097/WNR.0000000000000697

15. Pahapill PA, Lozano AM. The pedunculopontine nucleus and Parkinson's disease. *Brain*. 2000;123(Pt 9):1767-83.

16. Thevathasan W, Moro E. What is the therapeutic mechanism of pedunculopontine nucleus stimulation in Parkinson's disease? *Neurobiology of Disease*. Published online 2019. doi:10.1016/j.nbd.2018.06.014

17. Garcia-Rill E, Skinner RD, Fitzgerald JA. Activity in the mesencephalic locomotor

region during locomotion. *Exp Neurol*. 1983;82(3):609-622.

18. Takakusaki K, Oohinata-Sugimoto J, Saitoh K, Habaguchi T. Role of basal ganglia-brainstem systems in the control of postural muscle tone and locomotion. *Prog Brain Res*. 2004;143:231-237. doi:S0079-6123(03)43023-9 [pii] 10.1016/S0079-6123(03)43023-9

19. Roseberry TK, Lee AM, Lalive AL, Wilbrecht L, Bonci A, Kreitzer AC. Cell-Type-Specific Control of Brainstem Locomotor Circuits by Basal Ganglia. *Cell*. 2016;164(3):526-537. doi:10.1016/j.cell.2015.12.037

20. Sebille SB, Belaid H, Philippe AC, et al. Anatomical evidence for functional diversity in the mesencephalic locomotor region of primates. *Neuroimage*. 2017;147:66-78. doi:10.1016/j.neuroimage.2016.12.011

21. Dautan D, Kovács A, Bayasgalan T, Diaz-Acevedo MA, Pal B, Mena-Segovia J. Modulation of motor behavior by the mesencephalic locomotor region. *Cell Rep*. 2021;36(8):109594. doi:10.1016/j.celrep.2021.109594

22. Craig AD. How do you feel? Interoception: the sense of the physiological condition of the body. *Nat Rev Neurosci*. 2002;3(8):655-666. doi:10.1038/nrn894 nrn894 [pii]

23. Branco T, Redgrave P. The Neural Basis of Escape Behavior in Vertebrates. *Annu Rev Neurosci*. 2020;43:417-439. doi:10.1146/annurev-neuro-100219-122527

24. Grillner S, Shik ML. On the descending control of the lumbosacral spinal cord from the "mesencephalic locomotor region." *Acta Physiol Scand*. 1973;87(3):320-333. doi:10.1111/j.1748-1716.1973.tb05396.x

25. Ryczko D. The Mesencephalic Locomotor Region: Multiple Cell Types, Multiple Behavioral Roles, and Multiple Implications for Disease. *Neuroscientist*. 2024;30(3):347-366. doi:10.1177/10738584221139136

26. Martinez-Gonzalez C, Wang HL, Micklem BR, Bolam JP, Mena-Segovia J. Subpopulations of cholinergic, GABAergic and glutamatergic neurons in the pedunculopontine nucleus contain calcium-binding proteins and are heterogeneously distributed. *Eur J Neurosci*. 2012;35(5):723-734. doi:10.1111/j.1460-9568.2012.08002.x

27. Wang HL, Morales M. Pedunculopontine and laterodorsal tegmental nuclei contain distinct populations of cholinergic, glutamatergic and GABAergic neurons in the rat. *Eur J Neurosci*. 2009;29(2):340-358. doi:10.1111/j.1460-9568.2008.06576.x

28. Opris I, Dai X, Johnson DMG, et al. Activation of Brainstem Neurons During Mesencephalic Locomotor Region-Evoked Locomotion in the Cat. *Front Syst Neurosci*. 2019;13:69. doi:10.3389/fnsys.2019.00069

29. van der Zouwen CI, Tello AJ, Suresh JS, et al. Cell-type specific sensory and motor activity in the cuneiform nucleus and pedunculopontine nucleus in mice. *Sci Rep*. 2025;15(1):20408. doi:10.1038/s41598-025-05572-2

30. Masini D, Kiehn O. Targeted activation of midbrain neurons restores locomotor function in mouse models of parkinsonism. *Nat Commun*. 2022;13(1):504. doi:10.1038/s41467-022-28075-4

31. Norton JA, Mushahwar VK. Afferent inputs to mid- and lower-lumbar spinal segments are necessary for stepping in spinal cats. *Ann N Y Acad Sci*. 2010;1198:10-20. doi:10.1111/j.1749-6632.2010.05540.x

32. Goetz L, Piallat B, Bhattacharjee M, Mathieu H, David O, Chabardès S. Spike discharge characteristic of the caudal mesencephalic reticular formation and pedunculopontine nucleus in MPTP-induced primate model of Parkinson disease. *Neurobiology of Disease*. Published online 2019. doi:10.1016/j.nbd.2018.08.002

33. Karachi C, Grabli D, Bernard FA, et al. Cholinergic mesencephalic neurons are involved in gait and postural disorders in Parkinson disease. *J Clin Invest*. 2010;120(8):2745-2754. doi:42642 [pii] 10.1172/JCI42642

34. Shimamoto SA, Larson PS, Ostrem JL, Glass GA, Turner RS, Starr PA. Physiological identification of the human pedunculopontine nucleus. *J Neurol Neurosurg Psychiatry*. 2010;81(1):80-86. doi:10.1136/jnnp.2009.179069

35. Piallat B, Chabardes S, Torres N, et al. Gait is associated with an increase in tonic firing of the sub-cuneiform nucleus neurons. *Neuroscience*. 2009;158(4):1201-1205. doi:S0306-4522(08)01587-X [pii] 10.1016/j.neuroscience.2008.10.046

36. Chang SJ, Cajigas I, Guest JD, et al. MR Tractography-Based Targeting and Physiological Identification of the Cuneiform Nucleus for Directional DBS in a Parkinson's Disease Patient With Levodopa-Resistant Freezing of Gait. *Front Hum Neurosci*. 2021;15:676755. doi:10.3389/fnhum.2021.676755

37. Weinberger M, Hamani C, Hutchison WD, Moro E, Lozano AM, Dostrovsky JO. Pedunculopontine nucleus microelectrode recordings in movement disorder patients. *Exp Brain Res*. 2008;188(2):165-174. doi:10.1007/s00221-008-1349-1

38. Galazky I, Kaufmann J, Voges J, Hinrichs H, Heinze HJ, Sweeney-Reed CM. Neuronal spiking in the pedunculopontine nucleus in progressive supranuclear palsy and in idiopathic Parkinson's disease. *J Neurol*. 2019;266(9):2244-2251. doi:10.1007/s00415-019-09396-9

39. Yako T, Kitazawa K, Kobayashi S, et al. Role of Microelectrode Recording in Deep Brain Stimulation of the Pedunculopontine Nucleus: A Physiological Study of Two Cases. *Neuromodulation*. 2022;25(6):925-934. doi:10.1111/ner.13479

40. Tattersall TL, Stratton PG, Coyne TJ, et al. Imagined gait modulates neuronal network dynamics in the human pedunculopontine nucleus. *Nat Neurosci*. 2014;17(3):449-454. doi:nn.3642 [pii] 10.1038/nn.3642

41. Lau B, Welter ML, Belaid H, et al. The integrative role of the pedunculopontine nucleus in human gait. *Brain*. 2015;138(5). doi:10.1093/brain/awv047

42. Fraix V, Bastin J, David O, et al. Pedunculopontine nucleus area oscillations during stance, stepping and freezing in Parkinson's disease. *PLoS One*. 2013;8(12):e83919. doi:10.1371/journal.pone.0083919 PONE-D-13-31100 [pii]

43. Thevathasan W, Pogosyan A, Hyam JA, et al. Alpha oscillations in the pedunculopontine nucleus correlate with gait performance in parkinsonism. *Brain*. 2012;135(Pt 1):148-160. doi:awr315 [pii] 10.1093/brain/awr315

44. Molina R, Hass CJ, Sowalsky K, et al. Neurophysiological Correlates of Gait in the Human Basal Ganglia and the PPN Region in Parkinson's Disease. *Frontiers in Human Neuroscience*. Published online 2020. doi:10.3389/fnhum.2020.00194

45. He S, Deli A, Fischer P, et al. Gait-Phase Modulates Alpha and Beta Oscillations in the Pedunculopontine Nucleus. *J Neurosci*. 2021;41(40):8390-8402. doi:10.1523/JNEUROSCI.0770-21.2021

46. Goetz L, Bhattacharjee M, Ferraye MU, et al. Deep Brain Stimulation of the Pedunculopontine Nucleus Area in Parkinson Disease: MRI-Based Anatomoclinical Correlations and Optimal Target. *Clinical Neurosurgery*. Published online 2019. doi:10.1093/neuros/nyy151

47. Plaha P, Gill SS. Bilateral deep brain stimulation of the pedunculopontine nucleus for Parkinson's disease. *Neuroreport*. 2005;16(17):1883-1887.

48. Collomb-Clerc A, Yeche M, Demain A, et al. Subthalamic Electrophysiological Mapping of Gait Initiation Dynamics and Freezing in Parkinson's Disease. *Ann Neurol*. 2025;Jul 25. doi:10.1002/ana.70003

49. Molina R, Hass CJ, Cernera S, et al. Closed-Loop Deep Brain Stimulation to Treat Medication-Refractory Freezing of Gait in Parkinson's Disease. *Front Hum Neurosci*. 2021;15:633655. doi:10.3389/fnhum.2021.633655

50. Goetz CG, Tilley BC, Shaftman SR, et al. Movement Disorder Society-sponsored

revision of the Unified Parkinson's Disease Rating Scale (MDS-UPDRS): scale presentation and clinimetric testing results. *Mov Disord*. 2008;23(15):2129-2170. doi:10.1002/mds.22340

51. Sebille SB, Rolland AS, Welter ML, Bardinet E, Santin MD. Post mortem high resolution diffusion MRI for large specimen imaging at 11.7 T with 3D segmented echo-planar imaging. *J Neurosci Methods*. 2019;311:222-234. doi:10.1016/j.jneumeth.2018.10.010

52. Thomas M, Jankovic J, Suteerawattananon M, et al. Clinical gait and balance scale (GABS): validation and utilization. *J Neurol Sci*. 2004;217(1):89-99.

53. Kiehn O. Decoding the organization of spinal circuits that control locomotion. *Nat Rev Neurosci*. 2016;17(4):224-238. doi:10.1038/nrn.2016.9

54. Noga BR, Whelan PJ. The Mesencephalic Locomotor Region: Beyond Locomotor Control. *Front Neural Circuits*. 2022;16:884785. doi:10.3389/fncir.2022.884785

55. de Lima-Pardini AC, Coelho DB, Nucci MP, et al. Brain networks associated with anticipatory postural adjustments in Parkinson's disease patients with freezing of gait. *Neuroimage Clin*. 2020;28:102461. doi:10.1016/j.nicl.2020.102461

56. Nardone A, Schieppati M. Balance in Parkinson's disease under static and dynamic conditions. *Mov Disord*. 2006;21(9):1515-1520. doi:10.1002/mds.21015

57. Massion J. Movement, posture and equilibrium: interaction and coordination. *Prog Neurobiol*. 1992;38(1):35-56. doi:0301-0082(92)90034-C [pii]

58. Richard A, Van Hamme A, Drevelle X, Golmard JL, Meunier S, Welter ML. Contribution of the supplementary motor area and the cerebellum to the anticipatory postural adjustments and execution phases of human gait initiation. *Neuroscience*. 2017;358. doi:10.1016/j.neuroscience.2017.06.047

59. Vervoort G, Nackaerts E, Mohammadi F, et al. Which Aspects of Postural Control Differentiate between Patients with Parkinson's Disease with and without Freezing of Gait? *Parkinsons Dis*. 2013;2013:971480. doi:10.1155/2013/971480

60. Dijkstra BW, Gilat M, Cofré Lizama LE, et al. Impaired Weight-Shift Amplitude in People with Parkinson's Disease with Freezing of Gait. *J Parkinsons Dis*. 2021;11(3):1367-1380. doi:10.3233/JPD-202370

61. Miron-Shahar Y, Kantelhardt JW, Grinberg A, et al. Excessive phase synchronization in cortical activation during locomotion in persons with Parkinson's disease. *Parkinsonism Relat Disord*. 2019;65:210-216. doi:10.1016/j.parkreldis.2019.05.030

62. Shine JM, Handojoseno AMA, Nguyen TN, et al. Abnormal patterns of theta frequency oscillations during the temporal evolution of freezing of gait in Parkinson's disease. *Clin Neurophysiol*. 2014;125(3):569-576. doi:10.1016/j.clinph.2013.09.006

63. Nieuwboer A, Giladi N. Characterizing freezing of gait in Parkinson's disease: models of an episodic phenomenon. *Mov Disord*. 2013;28(11):1509-1519. doi:10.1002/mds.25683

64. Cowie D, Limousin P, Peters A, Day BL. Insights into the neural control of locomotion from walking through doorways in Parkinson's disease. *Neuropsychologia*. 2010;48(9):2750-2757. doi:S0028-3932(10)00203-4 [pii] 10.1016/j.neuropsychologia.2010.05.022

65. Galazky I, Zaehle T, Sweeney-Reed CM, et al. Neuronal oscillations of the pedunculopontine nucleus in progressive supranuclear palsy: Influence of levodopa and movement. *Clin Neurophysiol*. 2020;131(2):414-419. doi:10.1016/j.clinph.2019.11.033

66. Li M, Zhou M, Wen P, et al. The network of causal interactions for beta oscillations in the pedunculopontine nucleus, primary motor cortex, and subthalamic nucleus of walking parkinsonian rats. *Exp Neurol*. 2016;282:27-36. doi:10.1016/j.expneurol.2016.05.007

67. Stefani A, Grandi LC, Galati S. Deep brain stimulation of the pedunculopontine nucleus modulates subthalamic pathological oscillations. *Neurobiol Dis*. 2019;128:49-52. doi:10.1016/j.nbd.2018.11.006

68. Alegre M, Alonso-Frech F, Rodriguez-Oroz MC, et al. Movement-related changes in oscillatory activity in the human subthalamic nucleus: ipsilateral vs. contralateral movements. *Eur J Neurosci*. 2005;22(9):2315-2324. doi:EJN4409 [pii] 10.1111/j.1460-9568.2005.04409.x

69. Tan H, Fischer P, Shah SA, Vidaurre D, Woolrich MW, Brown P. Decoding Movement States in Stepping Cycles Based on Subthalamic LFPs in Parkinsonian Patients. *Conf Proc IEEE Eng Med Biol Soc*. 2018;2018:1384-1387. doi:10.1109/EMBC.2018.8512545

70. Zhao H, Hao S, Zhang P, et al. Cortical and Corticomuscular Beta-Gamma Phase-Amplitude Coupling During Different Locomotion States and the Effects of Levodopa in Parkinson's Disease. *Mov Disord*. Published online September 6, 2025. doi:10.1002/mds.70031

71. Pozzi NG, Canessa A, Palmisano C, et al. Freezing of gait in Parkinson's disease reflects a sudden derangement of locomotor network dynamics. *Brain*. Published online 2019. doi:10.1093/brain/awz141

72. Thenaisie Y, Lee K, Moerman C, et al. Principles of gait encoding in the subthalamic nucleus of people with Parkinson's disease. *Sci Transl Med*. 2022;14(661):eabo1800. doi:10.1126/scitranslmed.abo1800

73. Anidi C, O'Day JJ, Anderson RW, et al. Neuromodulation targets pathological not physiological beta bursts during gait in Parkinson's disease. *Neurobiology of Disease*. Published online 2018. doi:10.1016/j.nbd.2018.09.004

74. Storzer L, Butz M, Hirschmann J, et al. Bicycling suppresses abnormal beta synchrony in the Parkinsonian basal ganglia. *Ann Neurol*. 2017;82(4):592-601. doi:10.1002/ana.25047

75. Oswal A, Cao C, Yeh CH, et al. Neural signatures of hyperdirect pathway activity in Parkinson's disease. *Nature Communications*. Published online 2021. doi:10.1038/s41467-021-25366-0

76. Binns TS, Köhler RM, Vanhoecke J, et al. Shared pathway-specific network mechanisms of dopamine and deep brain stimulation for the treatment of Parkinson's disease. *Nat Commun*. 2025;16(1):3587. doi:10.1038/s41467-025-58825-z

77. Litvak V, Jha A, Eusebio A, et al. Resting oscillatory cortico-subthalamic connectivity in patients with Parkinson's disease. *Brain*. Published online 2010. doi:awq332 [pii] 10.1093/brain/awq332

78. Jacobs JV, Lou JS, Kraakevik JA, Horak FB. The supplementary motor area contributes to the timing of the anticipatory postural adjustment during step initiation in participants with and without Parkinson's disease. *Neuroscience*. 2009;164(2):877-885. doi:S0306-4522(09)01295-0 [pii] 10.1016/j.neuroscience.2009.08.002

79. Eidelberg E, Walden JG, Nguyen LH. Locomotor control in macaque monkeys. *Brain*. 1981;104(Pt 4):647-663.

80. Chang SJ, Santamaria AJ, Sanchez FJ, et al. Deep brain stimulation of midbrain locomotor circuits in the freely moving pig. *Brain Stimul*. 2021;14(3):467-476. doi:10.1016/j.brs.2021.02.017

81. Gatto G, Goulding M. Locomotion Control: Brainstem Circuits Satisfy the Need for Speed. *Curr Biol*. 2018;28(6):R256-R259. doi:10.1016/j.cub.2018.01.068

82. Fougère M, van der Zouwen CI, Boutin J, Neszvecsko K, Sarret P, Ryczko D. Optogenetic stimulation of glutamatergic neurons in the cuneiform nucleus controls locomotion in a mouse model of Parkinson's disease. *Proc Natl Acad Sci U S A*. 2021;118(43):e2110934118. doi:10.1073/pnas.2110934118

83. Matsuyama K, Drew T. Vestibulospinal and reticulospinal neuronal activity during locomotion in the intact cat. I. Walking on a level surface. *J Neurophysiol*. 2000;84(5):2237-2256.

84. Prentice SD, Drew T. Contributions of the reticulospinal system to the postural adjustments occurring during voluntary gait modifications. *J Neurophysiol*. 2001;85(2):679-98.

85. Goñi-Erro H, Selvan R, Caggiano V, Leiras R, Kiehn O. Pedunculopontine Chx10+ neurons control global motor arrest in mice. *Nat Neurosci*. 2023;26(9):1516-1528. doi:10.1038/s41593-023-01396-3

86. Thevathasan W, Coyne TJ, Hyam JA, et al. Pedunculopontine nucleus stimulation improves gait freezing in Parkinson disease. *Neurosurgery*. 2011;69(6):1248-1253; discussion 1254. doi:10.1227/NEU.0b013e31822b6f71

87. Roussel M, Lafrance-Zoubga D, Josset N, Lemieux M, Bretzner F. Functional contribution of mesencephalic locomotor region nuclei to locomotor recovery after spinal cord injury. *Cell Rep Med*. 2023;4(2):100946. doi:10.1016/j.xcrm.2023.100946

88. Hofer AS, Scheuber MI, Sartori AM, et al. Stimulation of the cuneiform nucleus enables training and boosts recovery after spinal cord injury. *Brain*. 2022;145(10):3681-3697. doi:10.1093/brain/awac184

89. Hofer AS, Stieglitz LH, Bolliger M, et al. Cuneiform Nucleus Stimulation Can Assist Gait Training to Promote Locomotor Recovery in Individuals With Incomplete Tetraplegia. *Ann Neurol*. Published online September 10, 2025. doi:10.1002/ana.78026

90. Little S, Pogosyan A, Neal S, et al. Adaptive deep brain stimulation in advanced Parkinson disease. *Ann Neurol*. 2013;74(3):449-457. doi:10.1002/ana.23951

91. Busch JL, Kaplan J, Behnke JK, et al. Chronic adaptive deep brain stimulation for Parkinson's disease: clinical outcomes and programming strategies. *NPJ Parkinsons Dis*. 2025;11(1):264. doi:10.1038/s41531-025-01124-7

92. Wilkins KB, Petrucci MN, Lambert EF, et al. Beta Burst-Driven Adaptive Deep Brain Stimulation Improves Gait Impairment and Freezing of Gait in Parkinson's Disease. *medRxiv*. Published online June 27, 2024:2024.06.26.24309418. doi:10.1101/2024.06.26.24309418

93. Louie KH, Balakid JP, Bath JE, et al. Adaptive deep brain stimulation timed to gait phase improves walking in Parkinson's disease. *medRxiv*. Published online August 21, 2025:2025.08.19.25333759. doi:10.1101/2025.08.19.25333759

94. Camastra C, Augimeri A, Quattrone A, Quattrone A. Unveiling the neural network of freezing of gait in Parkinson's disease: A coordinate-based network study. *J Parkinsons Dis*. 2025;15(5):982-989. doi:10.1177/1877718X251348669

95. Botta P, Fushiki A, Vicente AM, et al. An Amygdala Circuit Mediates Experience-Dependent Momentary Arrests during Exploration. *Cell*. 2020;183(3):605-619.e22. doi:10.1016/j.cell.2020.09.023

Figure legends

Figure 1 Anatomical reconstruction of DBS electrodes within the MLR. Upper panel: (A) 3D view of the locations of the left and right DBS electrodes in one PD patient, superimposed with the post-mortem brainstem atlas (grey), with the purple area corresponding to the location of the cholinergic neurons within the MLR, corresponding to the PPN, and the green area corresponding to the location of the GABAergic dorsal/posterior territory, corresponding to the putative CuN.[51] **(B)** Locations of dipoles used for LFP recordings, reported on 3-D posterior views after fusion with the 3-D MRI image and brainstem atlas. The light green and purple volumes outline the putative CuN and PPN territories, respectively. Each dot represents one LFP bipolar derivation (n=15 in the CuN and n=13 in the PPN), with left **(C)** and right **(D)** sagittal views. **Bottom panel:** Locations of DBS electrodes and VTA for PPN (orange) and CuN (green) DBS, reported on 3-D posterior views for each individual patient.

Alt-text: *Three-dimensional reconstruction of the mesencephalic locomotor region showing the anatomical locations of recording and stimulation sites. The pedunculopontine nucleus (PPN, purple) is located ventrally and the cuneiform nucleus (CuN, green) dorsally, within a histological atlas registered to each patient's MRI. Bilateral electrodes follow oblique trajectories traversing both nuclei. Recording dipoles assigned of the CuN and PPN are displayed on sagittal and posterior views, illustrating their spatial distribution across patients, with one dot per stimulation site. Additional panels (bottom) show the locations of stimulating contacts used for CuN-DBS and PPN-DBS, together with the corresponding stimulation amplitudes for each patient. The figure highlights the anatomical organisation of the mesencephalic locomotor regions and the clear separation between dorsal CuN and ventral PPN recording and stimulation sites.*

Figure 2 Multimodal profiling of MLR dynamics during gait initiation. (A) Schematic of the experimental setup combining simultaneous MLR-LFP recordings (via externalized DBS

leads) with whole-body motion capture, force platform dynamometry (Center of Pressure, CoP; Center of Mass, CoM), and surface electromyography (EMG) of soleus (SOL) and tibialis (TA). Temporal events are defined as: t0 (onset of anticipatory postural adjustment phase, APA), FO1 (foot-off, first step) and FO2 (foot-off, second step). **(B)** Reconstruction of leg kinematics in one patient for one trial without FOG (FOG-, upper panel) and one trial with FOG (FOG+, bottom panel, orange). **(C)** Baseline mesencephalic power spectra. Left: Mean power spectral density (PSD) at rest for CuN and PPN. Right: Comparison of average baseline power in the alpha (8–12 Hz) and low-beta (13–20 Hz) bands. Dots indicate patient-level averages across contacts (n = 4 patients). *p < 0.05, paired t-test.**(D)** Gait initiation mechanics with and without freezing. Box plots showing kinetic sub-scores, i.e. *Pace*, *Rhythm*, and *Lateral balance*, for trials with (FOG+) and without (FOG−) freezing episodes, in $DOPA^{OFF}$ and $DOPA^{ON}$ states. ***p<0.001, LMM, Bonferroni corrected. Box elements: center line, median; box limits, upper and lower quartiles; whiskers, 1.5 times interquartile range; dots, individual trials.

Alt-text: *Schematic representation of the experimental design. Patients performed repeated gait initiation trials while local field potentials were simultaneously recorded from the CuN and PPN. Biomechanical recordings included force-platform measurements of centre-of-foot-pressure displacement, three-dimensional kinematic tracking, and synchronized neural recordings, with analyses focused on alpha and beta-band activity. The gait initiation sequence is divided into anticipatory postural adjustments (APAs), first foot-off and first foot contact. Representative traces illustrate the temporal alignment between biomechanical events and mesencephalic neural activity. The figure also summarizes the decomposition of gait initiation into Pace, Rhythm and Lateral Balance components, and illustrates how trials followed by freezing of gait exhibit altered gait initiation performance.*

Figure 3 Spatiotemporal dissociation of CuN and PPN activity during gait initiation. (A) Time–frequency analysis of CuN and PPN activity. Spectrograms show grand averages event-related power modulations across trials and patients (relative to baseline) aligned with the onset of anticipatory postural adjustments (t0). The dashed vertical line indicates the average time of the first foot-off (FO1); the horizontal boxplot above illustrates the distribution of FO1 timings across all trials. Significant differences are outlined in black (p < 0.05, LMM). **(B)** Functional contrast map. Time-frequency plot illustrating the direct statistical comparison between PPN and CuN power modulation (PPN – CuN). Warm colors indicate higher power in CuN; cool colors indicate higher power in PPN. Significant differences are outlined in black (p < 0.05, LMM). **(C)** Frequency-specific temporal

dynamics. Averaged power modulation time-courses for the alpha (8–12 Hz) and low-beta (13–20 Hz) bands in the CuN (green) and PPN (purple). Black bars at the top indicate time points with significant divergence between the two nuclei ($p < 0.05$, LMM). Shaded areas represent standard error of the mean (SEM).

Alt-text: *Time-frequency maps and group analyses comparing neural activity in the CuN and PPN during gait initiation. CuN recordings show increased alpha-band activity preceding anticipatory postural adjustments, whereas PPN recordings exhibit prominent beta-band desynchronization during postural adjustments followed by alpha-band modulation during step execution. Line plots summarize changes in spectral power over time relative to gait events.*

Figure 4 Mesencephalic neural signatures of freezing vulnerability. (A) State-dependent spectral dynamics. Time-frequency maps showing LFP power modulation (relative to baseline) in the CuN and PPN, separately for effective gait initiation without subsequent freezing (FOG−, upper row) and trials where successful gait initiation led to freezing (FOG+, lower row). Data are aligned to the APA onset (t0). Statistical significance was assessed using LMMs ($p < 0.05$) and is indicated by black contours. **(B)** Collapse of functional segregation. Time-frequency plots showing the difference in power modulation between PPN and CuN (PPN - CuN) during FOG− and FOG+ trials. Significant spatial dissociation (black contours, $p < 0.05$) is prominent in FOG− trials but diminishes in FOG+ trials. **(C)** Frequency-specific breakdown. Temporal profiles of alpha (8-12 Hz) and low-beta (13-20 Hz) power modulation in CuN (green) and PPN (purple) for FOG− versus FOG+ conditions. Shaded areas represent SEM. Black bars indicate significant differences between nuclei ($p < 0.05$, LMM).

Alt-text: *Comparison of neural activity during gait initiation trials that were followed by freezing of gait (FOG+) versus trials without freezing (FOG−). Time-frequency representations reveal excessive and temporally abnormal alpha-band synchronisation across the mesencephalic locomotor region before freezing episodes. Additional abnormalities are observed in PPN-beta-band activity. Group analyses differences in oscillatory power between conditions and identify time windows associated with subsequent freezing. The figure demonstrates that freezing is preceded by disruption of normal CuN and PPN neural dynamics rather than a complete loss of locomotor activity.*

Figure 5 Alpha-band dynamics encode gait initiation quality. (A) Spectral correlates of gait mechanics. Time-frequency maps display the statistical relationship (LMM

coefficients) between LFP power in CuN (left column) and PPN (right column) and biomechanical scores: *Pace*, *Rhythm*, and *Lateral Balance*. Data are aligned to APA onset (t0). The horizontal boxplot above shows the distribution of first foot-off (FO1) times; the dashed vertical line marks the mean FO1. Warm colors indicate positive correlations; cool colors indicate negative correlations. Black contours outline significant clusters ($p < 0.05$, LMM). **(B)** Alpha-band specific encoding across MLR. Temporal profiles of the correlation between alpha power (8–12 Hz) and biomechanical scores. Shaded areas represent SEM. Black bars denote time points where the correlation strength significantly differs from zero ($p < 0.05$, LMM). **(C)** Alpha-band specific encoding for CuN and PPN. Temporal profiles of the correlation between alpha power (8–12 Hz) and biomechanical scores for CuN (green) and PPN (purple). Green and purple bars indicate time points during which the correlation is significant for CuN and PPN, respectively ($p < 0.05$). Shaded areas represent SEM. Black bars denote time windows where the correlation strength differs significantly between nuclei ($p < 0.05$, LMM).

Alt-text: *Scatter plots and regression analyses illustrating the relationships between mesencephalic locomotor region oscillatory activity and biomechanical measures of gait initiation. Increased alpha-band power in the CuN during APAs is positively associated with better gait rhythm and lateral balance performance. In contrast, alpha-band activity in the PPN is negatively associated with pace measure. During the subsequent foot-off phase, higher PPN alpha-band activity is negatively correlated with gait rhythm, indicating distinct temporal contributions of CuN and PPN activity to different components of gait initiation. Regression lines and confidence intervals illustrate the direction and strength of these associations.*

Figure 6 Mesencephalic alpha activity predicts differential response to MLR-DBS. (A) Differential clinical effects. Box plots showing changes in biomechanical gait initiation scores (*Pace*, *Rhythm*, and *Lateral Balance*) induced by DBS^{CuN} and DBS^{PPN} relative to DBS^{OFF} (data pooled across $DOPA^{OFF}$ and $DOPA^{ON}$ states). The CuN stimulation selectively improves *Rhythm*, whereas PPN stimulation worsens *Pace*. Box elements: center line, median; box limits, upper and lower quartiles; whiskers, 1.5 times interquartile range; dots, individual trials. $^{**}p < 0.01$, $^{***}p < 0.001$, LMM, Bonferroni-corrected. **(B)** Alpha-band activity as a predictor of clinical outcome. Regression plots showing the relationship between the *Rhythm* score under DBS and the amplitude of alpha-band power during gait initiation (measured without DBS). Stronger alpha modulation predicts worse *Rhythm* outcomes, suggesting it marks resistance to therapy.

Alt-text: *Box plots and correlation analyses showing the effects of deep brain stimulation of the CuN (DBS^{CuN}) and the PPN (DBS^{PPN}) on gait initiation performance, relative to DBS^{OFF}. CuN DBS selectively improves gait rhythm, whereas PPN DBS reduces forward propulsion (pace). Additional plots show that excessive mesencephalic alpha-band activity predicts poorer responsiveness to DBS.*

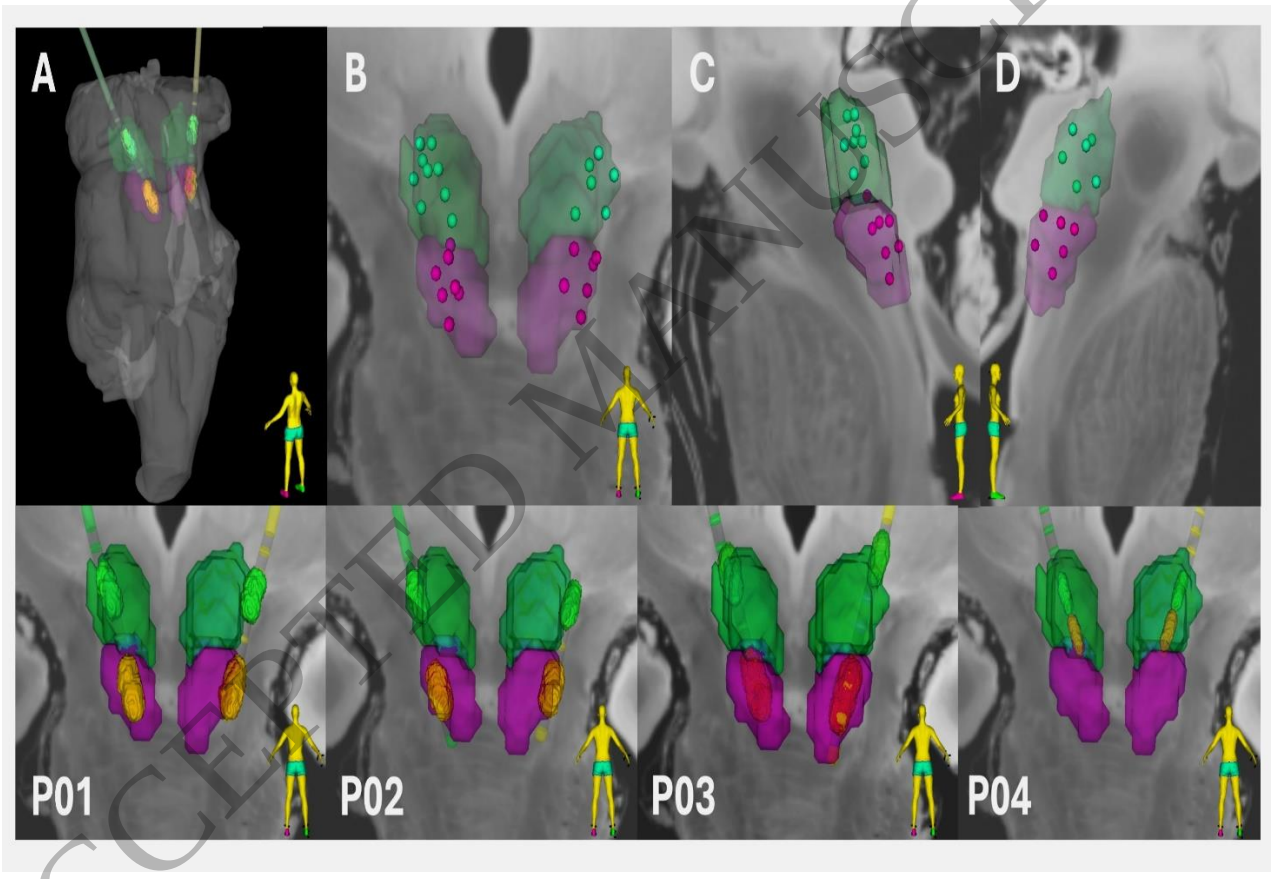

Figure 1
339x152 mm (x DPI)

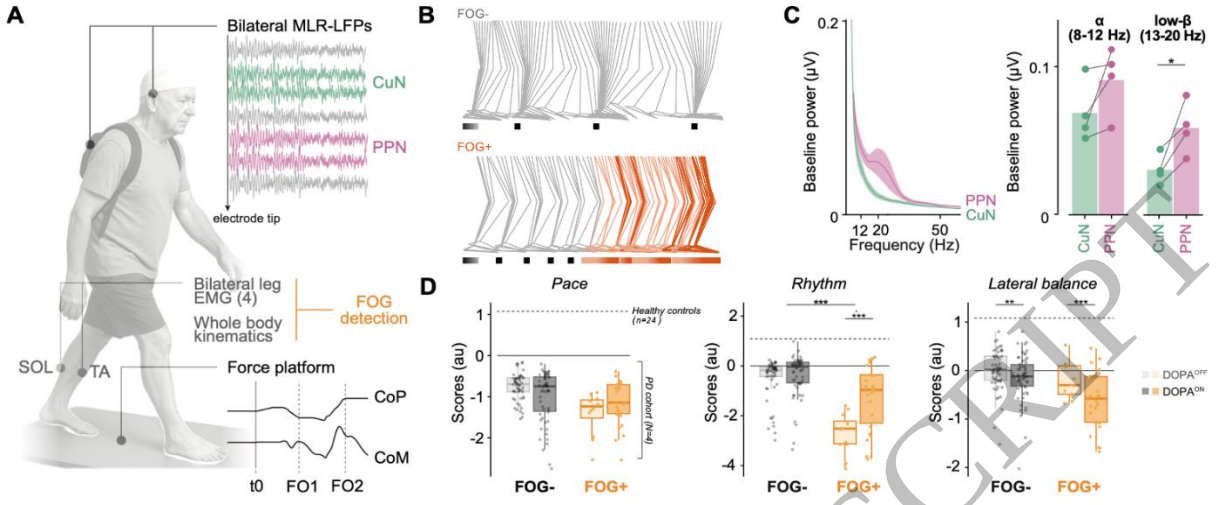

Figure 2
185x78 mm (x DPI)

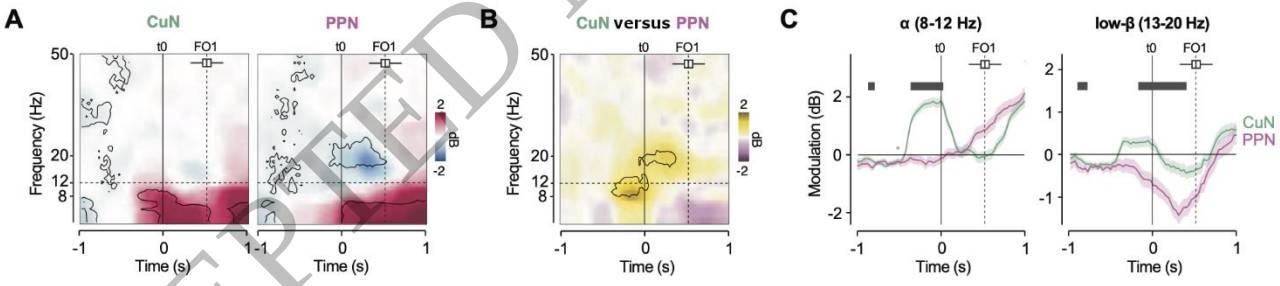

Figure 3
171x41 mm (x DPI)

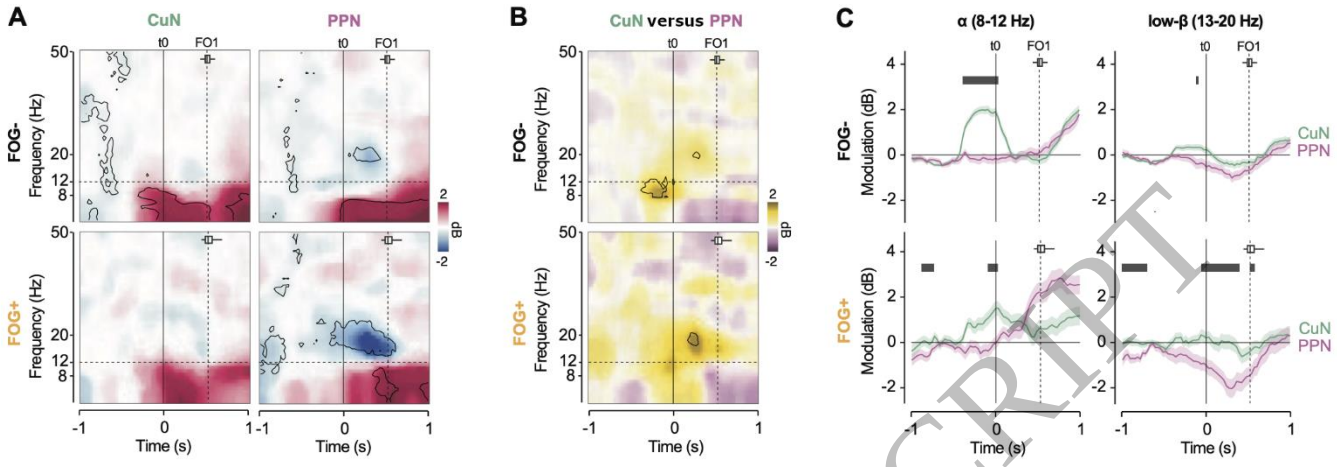

Figure 4
180x63 mm (x DPI)

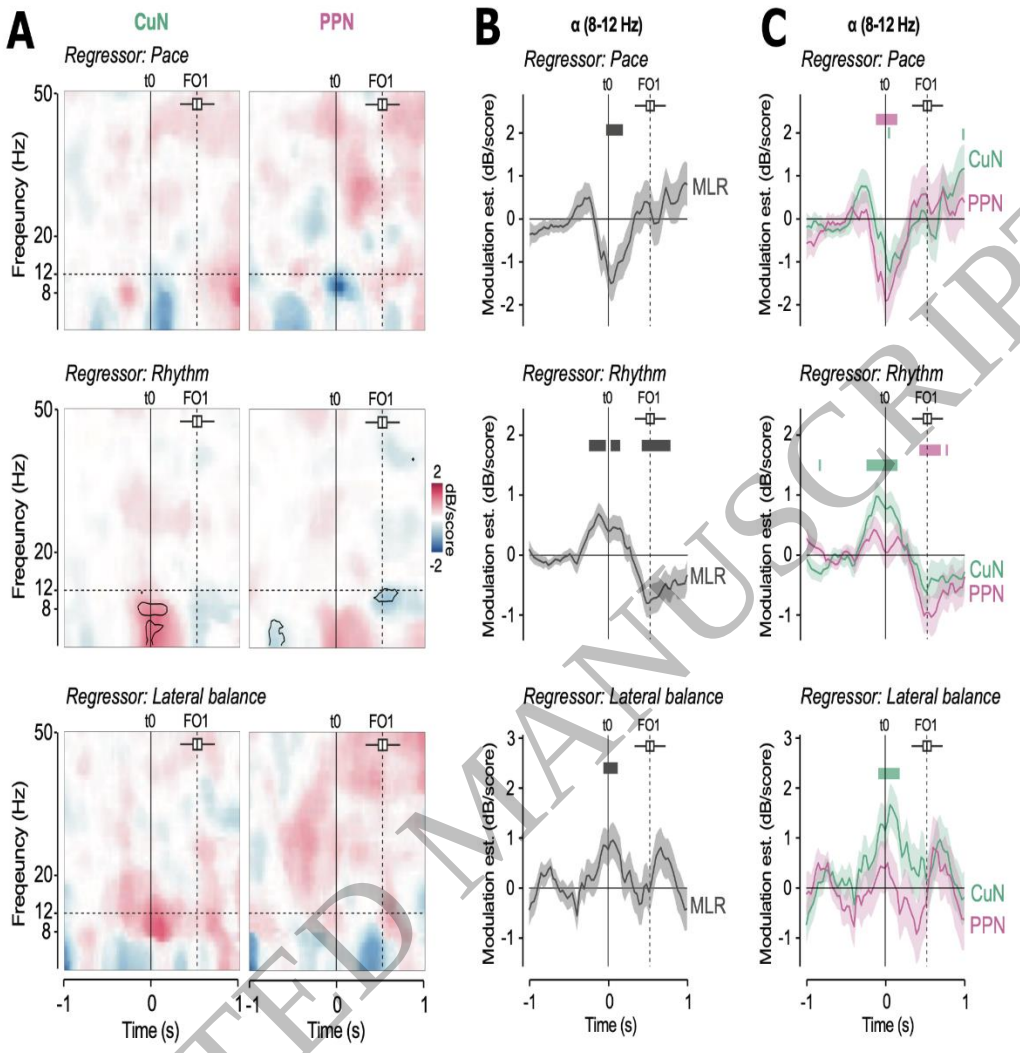

Figure 5
236x181 mm (x DPI)

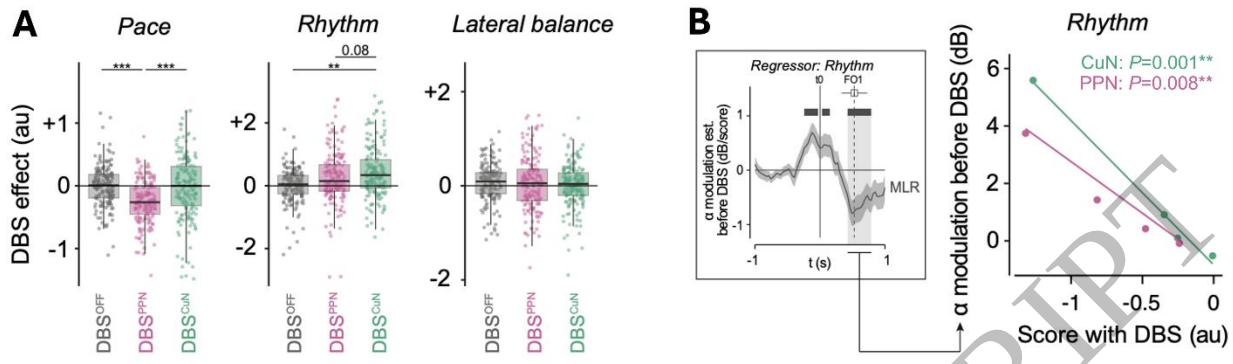

Figure 6
169x59 mm (x DPI)